UNDOPED AND Ni/Fe DOPED CuO NANOPARTICLES: A STRUCTURAL, OPTICAL, AND PHOTOCATALYTIC COMPARATIVE STUDY

N. Khlifi[1,2*], C. Zerrouki[2], N. Fourati [2], H. Guermazi[1] and S. Guermazi[1]

[1]Laboratory of Materials for Energy and Environment, and Modeling (LMEEM), Faculty of Sciences, University of Sfax, B.P: 1171, 3038, Tunisia. khlifinadia1991@gmail.com, hajer.guermazi@gmail.com, samir.guermazi@gmail.com
[2]Laboratories of Information and Energy Technology Systems and Applications (SATIE).UMR 8029, CNRS, ENS Paris-Saclay, Cnam, 292 rue Saint-Martin, 7503, Paris, France. zerrouki@cnam.fr, fourati@cnam.fr

***** Author to whom correspondence should be addressed; E-Mail: khlifinadia1991@gmail.com

ABSTRACT:

The present work outlines the co-precipitation synthesis of undoped and -doped CuO NPs with two transition metals (TM), iron (Fe) and nickel (Ni), their characterization, and then their use as photocatalysts for the degradation of pollutants. The structural, morphological, and optical properties of the synthesized CuO NPs are characterized using X-ray diffraction (XRD), Scanning Electron Microscopy (SEM), Energy Dispersive Spectroscopy (EDS) and UV–Visible Diffused Reflectance Spectroscopy (DRS), techniques. The photocatalytic activities of the prepared oxide powders are evaluated against methylene blue (MB) taken as a model pollutant in aqueous media. The photodegradation efficiency is estimated and compared to other recent works.

Keywords: CuO NPs, Transition Metal (TM), Doping, Photocatalytic activity.

1. INTRODUCTION

As a well-known global fact, the presence of toxic, non-biodegradable and harmful organic pollutants in soils, wastewater, and atmosphere has become an indisputable significant environmental problem. Among organic pollutants, methylene blue (MB) is one of the most studied organic dyes. It is toxic, non-biodegradable, and carcinogenic and can cause a serious threat to humans and animals [1-3] (Figure 1).

In response to these major environmental concerns, numerous researchers have been directed toward the synthesis of catalysts for the degradation of pollutants. Metal oxide nanoparticles (NPs) constitute a major part of these new catalysts. Several research have shown that CuO NPs, which can be synthesized at low cost, exhibit excellent catalytic activity, low toxicity, and can degrade various types of organic pollutants [4]. This oxide is considered as a type p semiconductor due to the presence of acceptor levels due to copper deficiencies; it has a band gap that can vary between 1.2–1.5 eV [5] depending on the preparation method [6].

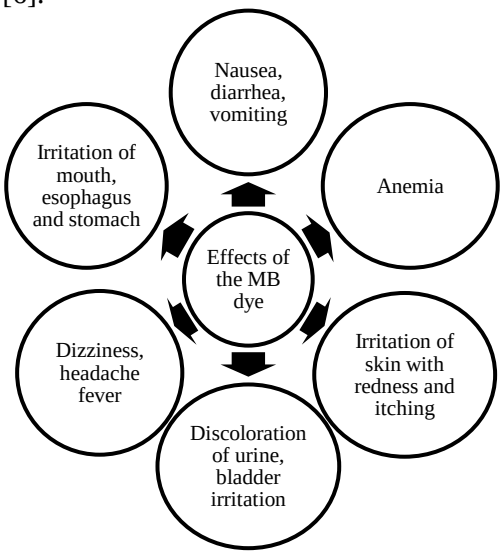

Figure 1: Harmful effects of MB dye

Modifying the physical and/or chemical properties of CuO NPs by cationic dopants is an approach that has been widely adopted in recent years to improve the catalytic activity [7, 8]. Inspired by this, we considered doping CuO with 2% iron and nickel, two transition metals (TM), before comparing their photocatalytic activity.

The three oxides NPs, CuO, CuO: Fe, and CuO: Ni, were characterized by means of XRD, SEM coupled with EDS, and DRS techniques. Then their photo-catalytic activities against MB were considered under solar irradiation.

2. DESCRIPTION OF THE WORK

2.1. EXPERIMENTAL

In this study, CuO, CuO:Ni and CuO:Fe NPs were synthesized via the co-precipitation method. The reagents were weighed to obtain the desired stoichiometric ratio and dissolved in distilled water. Then sodium hydroxide (NaOH) was added drop wise every 15 minutes to obtain the desired pH

value. The whole mixture was stirred for 3 hours at room temperature (25°C) using a magnetic stirrer to obtain a liquid solution. Rinses were carried out with distilled water and ethanol several times to remove any residues, and filtration was carried out using filter paper, as shown in Figure 2. The resulting paste was left to dry at 80°C for 12 hours to remove the water molecules, and then finely and uniformly ground to powder using an agate mortar. To obtain the final product (-doped and undoped coper oxides), the dry powder was calcined at 500°C for 4 hours, using an alumina crucible.

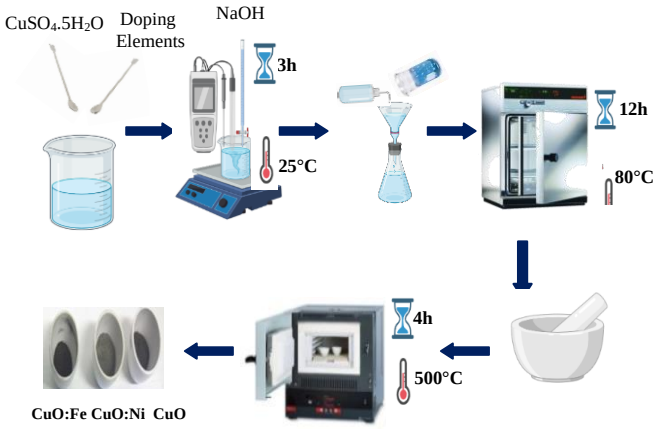

Figure 2: Schematic representation of the synthesis procedure by co-precipitation of undoped and -doped CuO NPs

2.2. RESULTS AND DISCUSSION

2.2.1. XRD ANALYSIS

The XRD patterns of the -doped and undoped CuO NPs are shown in Figure 3. For all samples, observed diffraction peaks correspond to the monoclinic structure, typical of Copper Oxide, with C2/c symmetry, according to the International Center for Diffraction Data (ICDD Card no. 01-089-2529) [9], and were assigned to the (110), (002), (111), (−202), (020), (202), (−113), (−311) and (113) planes. Furthermore, no secondary oxide phase is detected, indicating pure CuO phase formation, and the successful insertion of the doping elements in the CuO lattice.

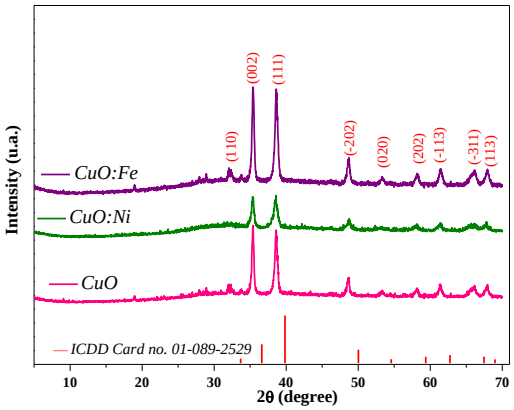

Figure 3: The XRD patterns of CuO, CuO:Fe and CuO:Ni NPs

2.2.2. SCANNING ELECTRON MICROSCOPE AND ENERGY DISPERSIVE SECTROSCOPY ANALYSIS

Scanning Electron Microscopy (SEM) was considered to access the morphology of the synthesized products. The images obtained (Figure 4) reveal for all three oxide samples an irregular distribution of particles whose size is difficult to estimate because of their strong agglomeration. Nickel doping seems to reduce the maximum size of agglomerated particles, compared to the case of undoped CuO. This trend is also observed in the case of Fe doping, with agglomerated particles being smaller in size than in the case of Ni.

The Energy Dispersive Spectroscopy (EDS) analysis was a non-destructive procedure to detect the elemental composition and purity of prepared samples.

The SEM images and EDS spectra of all samples have been shown in Figure 4.

The EDX spectrum shows a strong intense peak related to Cu and O atoms and less intense peak corresponding to Ni and Fe as doping element. Furthermore, the absence of peaks related to any impurities indicates the high elemental purity of synthesized samples.

The presence of the element Carbon (C) in the spectra of all samples is due to the substrate based on conductive carbon glue, used as a support during the analysis.

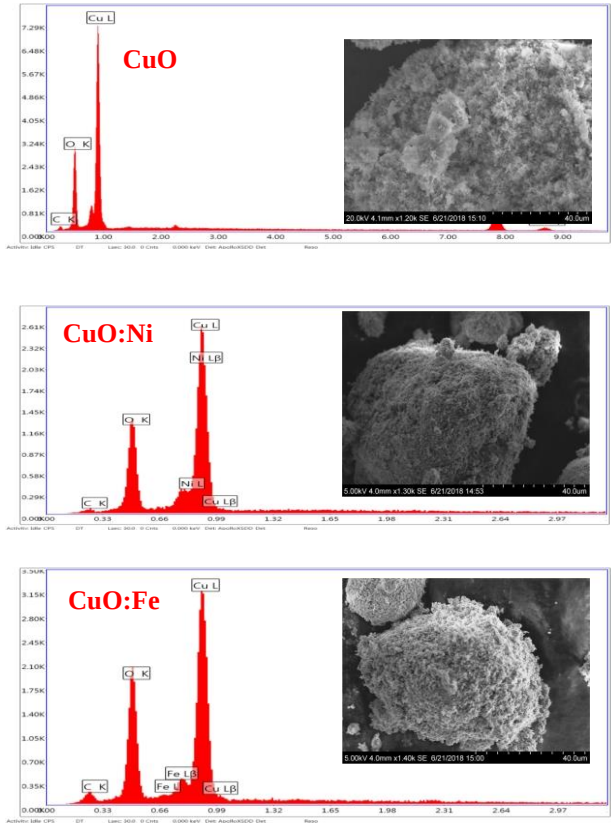

Figure 4: SEM and EDX-based analysis of undoped CuO, CuO:Ni and CuO:Fe NPs

At this stage, it is very important to have succeeded in doping with all the elements considered, allowing considering the photocatalytic tests in a comparative way with the undoped CuO.

2.2.3. UV–VIS DRS ANALYSIS

The direct transition of CuO NPs could not be investigated using the UV–Vis–NIR absorption spectroscopy because of weak absorption. Therefore, Diffused Reflectance Spectra (DRS) was used for the investigation of the doping effect on band gap energy of undoped and -doped CuO NPs with Ni and Fe are shown in Figure 5.

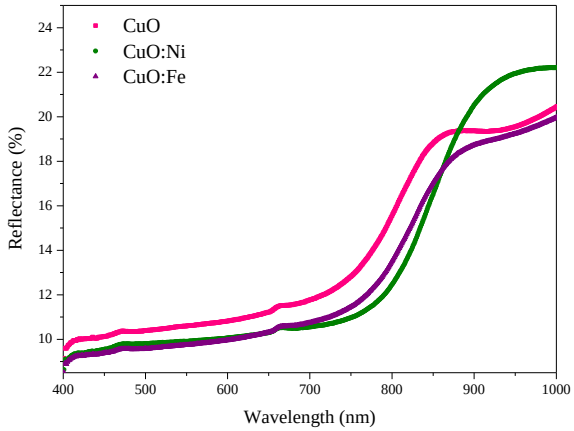

Figure 5: Diffused reflectance UV–Vis spectra of undoped and -doped CuO NPs

Figure 5 exhibits the comparison between the typical diffused reflectance spectra of CuO, CuO:Ni and CuO:Fe NPs in between 400 and 1000 nm wavelength region.

The absorption edge of undoped CuO was observed around 800 nm which was red shifted with different doping elements.

Low reflectance in visible range (400 - 800 nm) confirming high absorbance behavior in the solar spectrum region. The high absorbance of light in the visible region ranging from 400 to 800 nm indicates the applicability of using undoped and -doped CuO NPs as an absorbing material in solar cell [10].

The latter is estimated based on the well-established Kubelka-Munk (K-M) function F(R) (equation (1)):

$$F(R) = \frac{(1-R)^2}{2R} \quad (1)$$

Where R is the reflectance value.

The Eg value can be obtained from extrapolating the straight-line portions of the curves the $(F(R)\ h\nu)^2$ versus hν (eV) plot (case of indirect band gap), as shown in Figure 6.

CuO doping led to a slight decrease in the gap value, from 1.44 eV for the undoped oxide to 1.40 eV for CuO:Ni (reduction of the order of 2.3%) and to 1.41 eV for CuO:Fe (diminution of the order of 1.5%). All values remain in the interval 1.0 eV - 1.9 eV, reported for copper oxide particles [11].

This slight decrease of the band gap could be attributed on the one hand to the fact that Fe and Ni ions introduce additional energy levels near the valence band of CuO, and on the other hand to the interactions between the 4s and 4p orbitals of the CuO conduction band and the 3d orbitals of the dopant element [10].

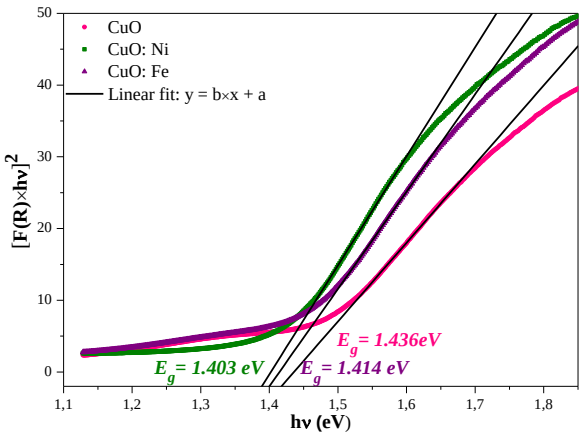

Figure 6: Variation of modified K-M function: $(F(R)\ h\nu)^2$ versus hν (eV), for undoped/-doped CuO NPs

2.2.4. PHOTOCATALYTIC ACTIVITY

To study the photocatalytic activity of undoped and Fe/Ni-doped CuO, we considered MB as a model pollutant and evaluated its photodegradation rate under sunlight irradiation. The tests were conducted on aqueous solution of 10 mg/L MB containing 30 mg of catalyst.

In order to reach the absorption/desorption equilibrium between the MB dye molecules and the catalyst surface of NPs, the solution was stirred for about 1 hour at room temperature in the dark, before exposed to the sun irradiation.

To evaluate the efficiency of degradation activities of the prepared samples, the decomposition of MB in dark and under sun light irradiation without catalyst was investigated (Figure 7 (a)).

It can be seen from Figure 7 (a) that the MB dye removal efficiency without the presence of NPs in a dark and even under sun light irradiation was negligible which is consistent with previously reported literature data [12, 13].

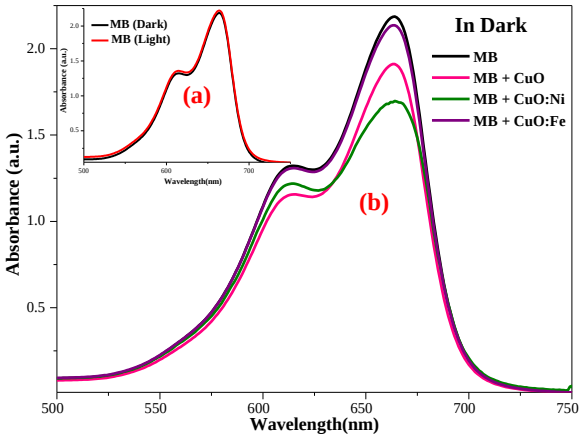

Figure 7: UV–Vis spectra of (a). MB in dark and under sun light irradiation, (b) MB with and without catalyst without irradiation

As shown in Figure 7 (a), a concentration of 10mg/L of MB without catalyst does not generate any transformation. But after addition of the catalyst NPs, the absorbance has been decreased even without light (Figure 7 (b)). This shows the beneficial effect of undoped and -doped CuO NPs and its power to degrade the MB dye.

After ensuring that there was no self-degradation of MB under solar irradiation, the effect of irradiation time was the predominant factor to determine the degradation capacity of NPs. So, we recorded absorbance spectra every half hour until 3 hours total irradiation time.

The results obtained (Figure 8) highlighted the absorbance decreases with the duration of sun exposure.

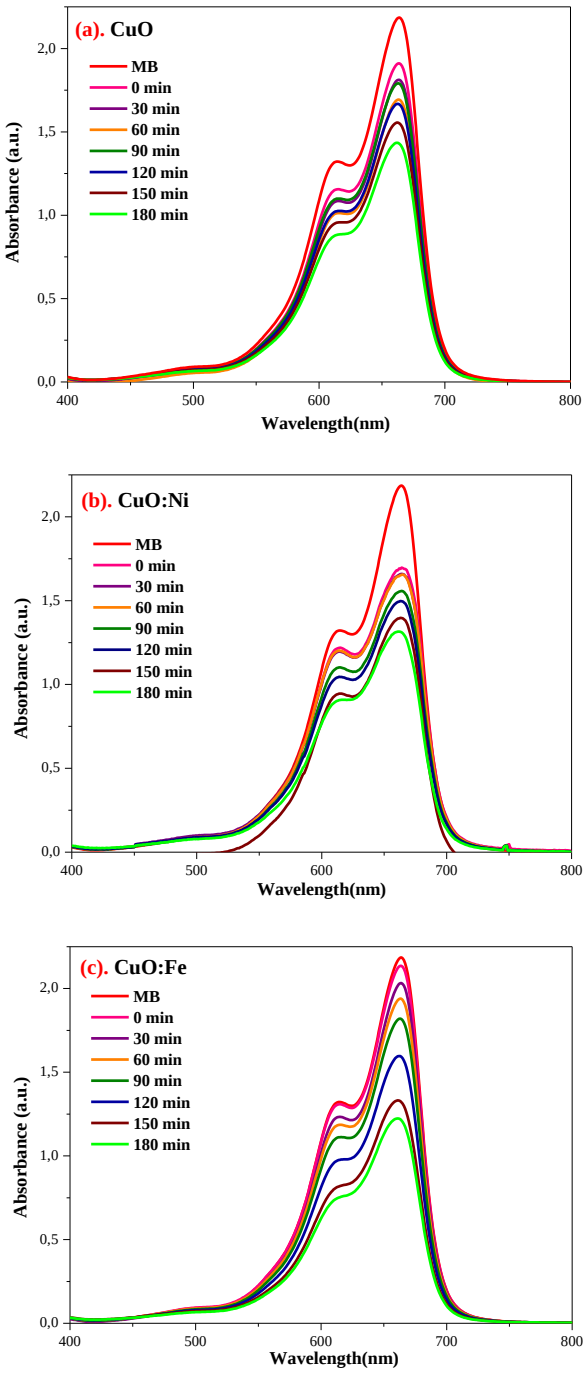

Figure 8: Photocatalytic degradation spectrum obtained using; (a) CuO; (b) CuO:Ni; and (c) CuO:Fe NPs

To compare the efficiency of the 3 catalysts, we calculated the degradation efficiency (% D), which represents the difference between the initial absorption peak of the MB dye and the final absorption peak, according to the following relationship (equation (2)):

$$\% D = \frac{A_0 - A_t}{A_0} \times 100 \quad (2)$$

Where A_0 is the dye absorbance without catalyst, and A_t is the absorbance of dye solution with catalyst after a time t.

The obtained results, gathered on Figure 9, show that iron doping substantially improves the photodegradation efficiency of CuO NPs.

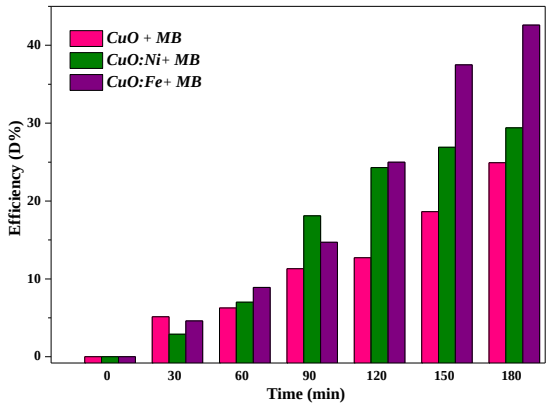

Figure 9: MB degradation efficiency of CuO, CuO:Ni and CuO:Fe NPs under solar-light irradiation

For comparison, we have collected in Table 1 some results from the literature concerning the efficiency of photocatalytic degradation of MB, and those we have obtained in this study.

Table 1: Comparison of degradation efficiencies of methylene blue dye using undoped/-doped CuO.

photocatalyst	Dye	Time (min)	D (%)	[Ref]
CuO	MB	80	25	[14]
CuO (pure) CuO:6% Fe	MB	240	44 40	[15]
Ni doped CuO	MB	420	80	[16]
CuO	MB	150	14.19	[17]
CuO CuO:Ni CuO:Fe	MB	180	24.92 29.4 42.6	This work

Our results, especially those with CuO:Fe, are among the best, with a relatively lower irradiation time. This is encouraging to continue in this direction, either by testing different doping rates, or by varying the nature of the dopants, or even considering composites with multi-doping.

3. PHOTOCATALYTIC MECHANISM

To explain the photodegradation mechanisms of MB dye, in the presence of CuO NPs, we have schematically gathered the different processes in Figure 10.

Under solar irradiation, the electrons (e^-) available in the valence band (VB) of the catalyst, acquire sufficient energy to pass into the conduction band (CB) (equation (3)). Once in the CB, the e^- reacts with the atmospheric oxygen (O_2) to produce the highly reactive super oxide anion (O_2^-) (equation (4)).

Concurrently, the holes (h^+) created in the BV, react with the water molecules (H_2O) to produce the hydroxyl radical ($OH^\bullet$), that possess strong oxidizing property (equation (5)).

Finally, $OH^\bullet$ and O_2^- contribute synergistically to degrade and mineralize the MB dye due to their higher reactive nature and produce non-toxic by-products like CO_2 and H_2O (equation (6)) [18].

$$CuO + h\upsilon \rightarrow (CB)e^- + (VB)h^+ \quad (3)$$

$$O_2 + (CB)e^- \rightarrow O_2^- \quad (4)$$

$$H_2O + (VB)h^+ \rightarrow H^+ + OH^\cdot \quad (5)$$

$$OH^\cdot / O_2^- + \text{MB dye} \rightarrow \text{By} - \text{products}\ (CO_2 + H_2O) \quad (6)$$

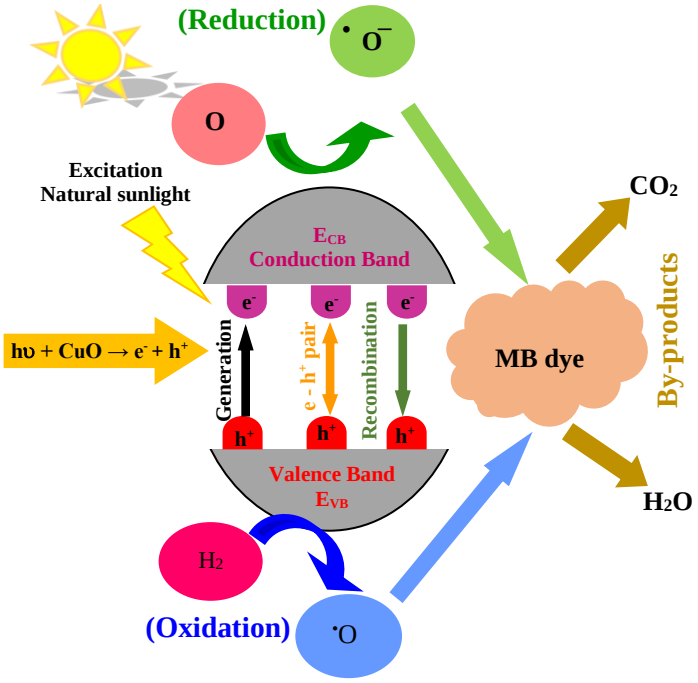

Figure 10: Photocatalytic mechanism of MB photodegradation, using CuO NPs as catalyst

4. SUMMARY

Undoped and -doped CuONPs were synthesized via the co-precipitation method. The properties of the as synthesized NPs are studied by XRD, SEM, EDS and UV-visible (DRS). The phase purity, morphology and optical properties of the powders varied upon changing the doping element. Besides, all the synthesized samples showed important photo-catalytic activity against MB. A significant improvement is obtained with CuO:Fe. The above encouraging results suggest continuing our investigations by considering the two routes mentioned before, i.e.:*i*) testing different doping rates and/or *ii)* varying the nature of the dopants.

5. REFERENCES

[1] Sun, L., Hu, D., Zhang, Z., & Deng, X. (2019). Oxidative Degradation of Methylene Blue via PDS-Based Advanced Oxidation Process Using Natural Pyrite. International Journal of Environmental Research and Public Health, 16(23), 4773.
DOI: 10.3390/ijerph16234773

[2] Contreras, M., Grande-Tovar, C. D., Vallejo, W., & Chaves-López, C. (2019). Bio-Removal of Methylene Blue from Aqueous Solution by Galactomyces geotrichum KL20A. Water, 11(2), 282.
DOI: 10.3390/w11020282

[3] Shakoor, S., & Nasar, A. (2017). Adsorptive treatment of hazardous methylene blue dye from artificially contaminated water using cucumis sativus peel waste as a low-cost adsorbent. Groundwater for Sustainable Development, 5, 152–159.
DOI: 10.1016/j.gsd.2017.06.005

[4] Pakzad, K., Alinezhad, H., & Nasrollahzadeh, M. (2019). Green synthesis of Ni@Fe_3O_4 and CuO nanoparticles using Euphorbia maculata extract as photocatalysts for the degradation of organic pollutants under UV-irradiation. Ceramics International.
DOI: 10.1016/j.ceramint.2019.05.27

[5] Rao, M. P., Sathishkumar, P., Mangalaraja, R. V., Asiri, A. M., Sivashanmugam, P., &Anandan, S. (2018). Simple and low-cost synthesis of CuO nanosheets for visible-light-driven photocatalytic degradation of textile dyes. Journal of Environmental Chemical Engineering, 6(2), 2003–2010.
DOI: 10.1016/j.jece.2018.03.008

[6] Botsa, S.M., R. Dharmasoth, and K. Basavaiah, A facile synthesis of Cu_2O and CuO nanoparticles via sonochemical assisted method. Current Nanoscience, 2019. **15**(2): p. 209-21.
DOI: 10.2174/1573413714666180530085447

[7] Pramothkumar, A., Senthilkumar, N., Mercy Gnana Malar, K. C., Meena, M., &VethaPotheher, I. (2019). A comparative analysis on the dye degradation efficiency of pure, Co, Ni and Mn-doped CuO nanoparticles. Journal of Materials Science: Materials in Electronics.
DOI: 10.1007/s10854-019-02262

[8] Pugazhendhi, A., Kumar, S. S., Manikandan, M., & Saravanan, M. (2018). Photocatalytic properties and antimicrobial efficacy of Fe doped CuO nanoparticles against the pathogenic bacteria and fungi. Microbial Pathogenesis, 122, 84–89.
DOI: 10.1016/j.micpath.2018.06.016

[9] Calos, N. J., Forrester, J. S., & Schaffer, G. B. (1996). A Crystallographic Contribution to the Mechanism of a Mechanically Induced Solid State Reaction. Journal of Solid State Chemistry, 122(2), 273–280.
DOI: 10.1006/jssc.1996.0113

[10] Naveena, D., Dhanabal, R., & Bose, A. C. (2022). Investigating the effect of La doped CuO thin film as absorber material for solar cell application. Optical Materials, 127, 112266.
DOI: doi.org/10.1016/j.optmat.2022.112266

[11] Iqbal, M., Ali, A., Ahmad, K. S., Rana, F. M., Khan, J., Khan, K., & Thebo, K. H. (2019). Synthesis and characterization of transition metals doped CuO nanostructure and their application in hybrid bulk heterojunction solar cells. SN Applied Sciences, 1(6).
DOI:10.1007/s42452-019-0663-5

[12]. M. Rashad, N.M. Shaalan & Alaa M. Abd-Elnaiem (2016) Degradation enhancement of methylene blue on ZnO nanocombs synthesized by thermal evaporation technique, Desalination and Water Treatment, 57:54, 2626726273.
DOI: 10.1080/19443994.2016.1163511.

[13]. Vasiljevic, Z. Z., Dojcinovic, M. P., Vujancevic, J. D., Jankovic-Castvan, I., Ognjanovic, M., Tadic, N. B., … Nikolic, M. V. (2020). Photocatalytic degradation of methylene blue under natural sunlight using iron titanate nanoparticles prepared by a modified sol–gel method. Royal Society Open Science, 7(9), 200708.
DOI: 10.1098/rsos.200708

[14] Oliveira, M. C., Fonseca, V. S., Neto, N. F. A., Ribeiro, R. A. P., Longo, E., de Lazaro, S. R., … Bomio, M. R. D. (2019). Connecting theory with experiment to understand the photocatalytic activity of CuO–ZnO heterostructure. Ceramics International.
DOI: 10.1016/j.ceramint.2019.12.20

[15] El Sayed, A. M., & Shaban, M. (2015). Structural, optical and photocatalytic properties of Fe and (Co, Fe) co-doped copper oxide spin coated films. Spectrochimica Acta Part A: Molecular and Biomolecular Spectroscopy, 149, 638–646.
DOI: 10.1016/j.saa.2015.05.010

[16] Shahzad, K., Karim, I., Abbass, S. M., Karim, H. K. H., Hussain, S., Ashfaq, M., & Rehman, M. (2020). Synthesis, Characterization, and Photocatalytic Degradation of Nickel Doped Copper Oxide Nanoparticles. Lahore Garrison University Journal of Life Sciences, 4(02), 130-138.
DOI: 10.54692/lgujls.2019.040210

[17] Velliyan, S., & Murugesan, K. S. (2022). Synthesis and study on structural, morphological, optical properties and photocatalytic activity of CuO: Erx3+ photocatalysts. Chinese Journal of Physics, 77, 2425-2434.
DOI: 0.1016/j.cjph.2022.04.024

[18] George, A., Magimai Antoni Raj, D., Venci, X., Dhayal Raj, A., Albert Irudayaraj, A., Josephine, R. L., Kaviyarasu, K. (2022). Photocatalytic effect of CuO nanoparticles flower-like 3D nanostructures under visible light irradiation with the degradation of methylene blue (MB) dye for environmental application. Environmental Research, 203, 111880.
DOI: 10.1016/j.envres.2021.111880